Real-time wall conditioning and recycling modification utilizing boron and boron nitride powder injections into the Large Helical Device

R. Lunsford[1], S. Masuzaki[2,3], F. Nespoli[1], N. Ashikawa[2,3], E. P. Gilson[1], D. A. Gates[1], K. Ida[2,3], G. Kawamura[2,3], T. Morisaki[2,3], A. Nagy[1], T. Oishi[2,3], M. Shoji[2], C. Suzuki[2,3], M. Yoshinuma[2]

[1] Princeton Plasma Physics Laboratory (PPPL) Princeton NJ 08543, USA
[2] National Institute for Fusion Science (NIFS) Toki, 509-5292, Gifu, Japan
[3] The Graduate University for Advanced Studies, SOKENDAI, Toki, 509-5292, Gifu, Japan

Controlled particulate injections from the PPPL Impurity Powder Dropper(IPD) into the Large Helical Device (LHD) have demonstrated positive effects on the wall conditions in both an intra and inter-shot basis. Injections over a range of densities, input powers, pulse lengths, heating schemes, injection quantities and main ion species show conclusive evidence of improvement to plasma wall conditions. Successful injections are confirmed by both spectroscopic measurements as well as real-time visible camera signals. In 7s long plasmas the responses include a reduction in wall recycling as well as a reduction in native impurity content as observed over the course of several discharges. For plasmas longer than 40s, improvements to the recycling rate and increased impurity control are observed in real time as a consequence of the extended particulate injections. These experiments demonstrate the extended applicability of this solid particulate conditioning technique to the control and maintenance of the plasma wall conditions. In addition they are an important initial step in the development of the real time boronization technique as a supplement to standard conditioning scenarios.

1. Introduction

The expected operational mode of a DEMO scale prototype fusion reactor[1-4] is that of steady state, near continuous operation. To that end, the plasma performance cannot become significantly degraded due to the evolution of adverse wall conditions. Thus, a need exists to develop methods capable of replenishing and refurbishing wall conditions during the operational phase of said device. In addition, the utilization of continuously operational superconducting magnets on projected next step long pulse fusion devices presents a challenge to the present methodologies of ensuring premium wall conditions through inter-discharge cleaning sessions. These strong steady state fields preclude the utilization of a nominal application of “glow discharge cleaning”[5] as well as placing programmatic limitations on the utilization of volume breakdown depositional methods such as boronization[6]. Given that standard boronization techniques in a superconducting device involve a cycling of the current within the cryogenic magnets to permit a volume breakdown, and that this procedure also entails an evacuation of the facility due to the toxic and explosive nature of any of a number of boron containing gasses such as diborane, the

development of an alternate method of replenishing the boronization coating would be programmatically very interesting. Indeed, if the number of these magnet cycles could be minimized by extending the operational time between boronizations there would be a substantial programmatic benefit in extended operational periods as well as enhanced component lifetimes.

In addition, even the present planned methods for maintaining optimal wall conditions in superconducting tokamaks face limitations as discharge lengths are increased. The utilization of Ion Cyclotron Wall Conditioning(ICWC) as tested on EAST[7] and Electron Cyclotron Wall Conditioning(ECWC) as used on JT60U[8] and planned for JT60SA[9] are techniques which are compatible with steady state magnetic fields and have been integrated into the ITER baseline for wall conditioning[10]. However these methodologies are operated in a "between-shots" basis and could not be utilized if wall conditions are observed to degrade significantly during extreme long pulse discharges. Thus a need also exists for a wall conditioning technique which can be utilized during the operational phase of a fusion research plasma.

The application of sub-millimeter powders have been observed to benefit the plasma material interface with both immediate and multi-discharge positive effects on plasma performance[11]. The injection of boron and boron nitride into active discharges provides an efficient way to transport coating materials to the surfaces of enhanced plasma contact where standard coating applications are most easily worn away such as the limiter and divertor surfaces. As such, the gravitational introduction of aerosolized boron containing compounds has been advocated as a real time wall conditioning technique and has been shown to positively impact the plasma material interface on DIII-D[12], ASDEX[13], EAST[14], and KSTAR[15]. The utilization of the solid particulate conditioning method has also resulted in immediate boosts in plasma performance in many cases[16-18]. This also includes recently reported confinement enhancements seen to accompany injections in LHD[19].

In this paper we summarize the results of multiple series of powder injection experiments. Taking advantage of the unique long pulse aspects and performance benchmarks of the LHD research program we explore the efficacy of the particulate conditioning technique over an extended parameter set. These parameters include variations in the discharge length, fill gas, plasma heating method, density and injection quantity. Positive plasma response over this extended parameter set provides a preliminary assessment of the viability of this technique in future fusion reactors. After briefly introducing the Impurity Powder Dropper as well as the LHD facility, the experiments are described and the observed results of powder injection are detailed. This includes both the prompt effects as well as an exploration of the long term conditioning effects observed through powder injection.

2. Experimental Apparatus

2.1 IPD

The Impurity Powder Dropper(IPD), shown in panel a) of figure 1 is installed in section 2.5 on the top of LHD. Panel b) of the same figure shows an image of the installation, while panel c) displays a

representative cutaway drawing of the IPD with panels d) and e) showing closeup images of typical dropper head components. The IPD, as described in more detail within Ref[20] contains four independent powder feeders arranged at 90 degree intervals around a central drop tube. Each dropper head is capable of independent operation, either individually or in concert with the others, providing a large number of possible powder combinations and concentrations.

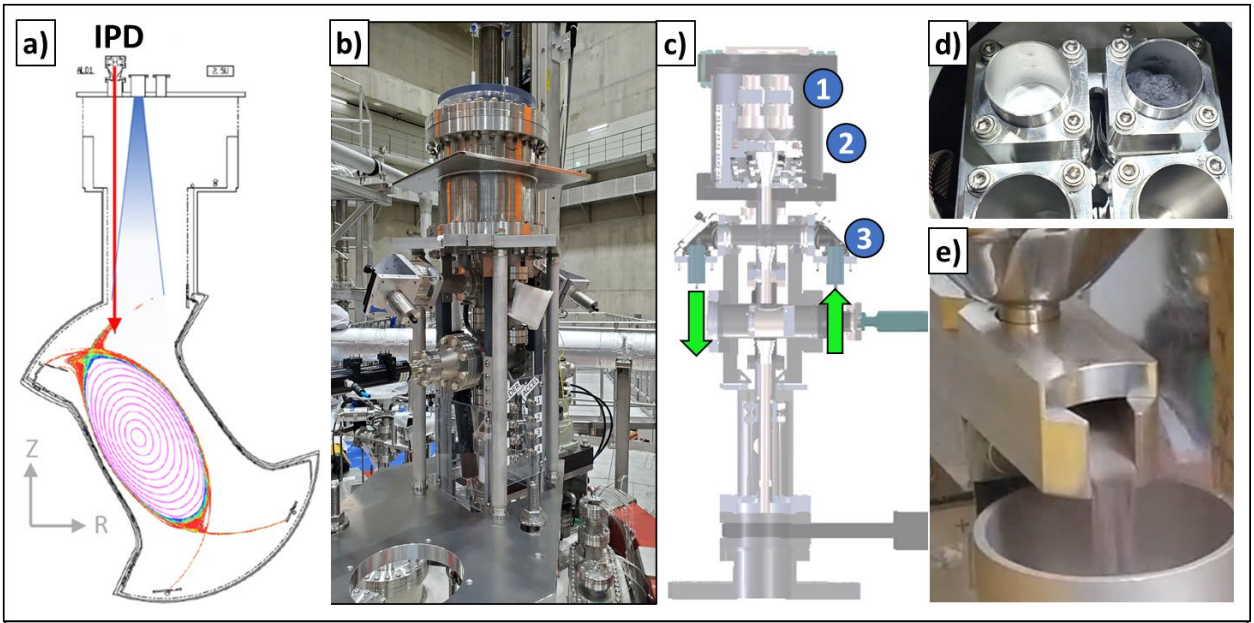

Figure 1 : Impurity Powder Dropper (IPD) apparatus and installation location. Panel a) shows the port location of the impurity powder dropper and its relation to the plasma below. The blue shaded region indicates the field of view of an injection camera. Panel b) shows an image of the IPD as installed on LHD with a cutaway drawing displayed in panel c). The numbers 1 – 3 indicate the powder reservoir, piezoelectric vibration stages and the flowmeter locations respectively where an image of the reservoir is shown in panel d) and a representative image of the powder flow from the front of the piezoelectric vibration stage is seen in panel e). The green arrows indicate the direction of light trave through the optical flowmeter.

Dropper operation is started by issue of an IPD control signal as shown in panel a) of figure 2 with the amplitude of said control signal proportional to operational voltage of the IPD. This in turn starts dropper vibration as monitored by onboard accelerometers. The falling powder, having being driven off of the feed tray is accelerated down a vertical drop tube. During the transit it passes through a collimated fiber-fed LED source. Occultation of this light by the transiting powder blocks a portion of the signal from reaching the corresponding photodiode on the other side of the drop tube resulting in a decrease in the signal as shown in panel b). This signal along with an accelerometer attached to the feeder tray provide a record of the duration and intensity of the powder injection. The time between the activation of the IPD and the subsequent drop in flowmeter signal is due to the powder transit time down the body of the IPD. This lag between activation of the IPD and introduction of material into the plasma is then further extended by the 2m drop between IPD flange and plasma location which the powder must transit. Thus any desired effects on the plasma must be anticipated by at least 1s to allow the powder time to reach

the plasma. In addition, random collisions between the falling powder will extend the falling path of certain particulates. This has the effect of extending the duration of an active injection pulse by up to an additional second. This can be observed in panels c) - e) of figure 2 where the despite the IPD being activated at t=3s, powder is not observed within LHD until after t=4s, and while the dropper excitation is stopped just after 7s, powder is still being introduced into the vessel after t = 8.5s

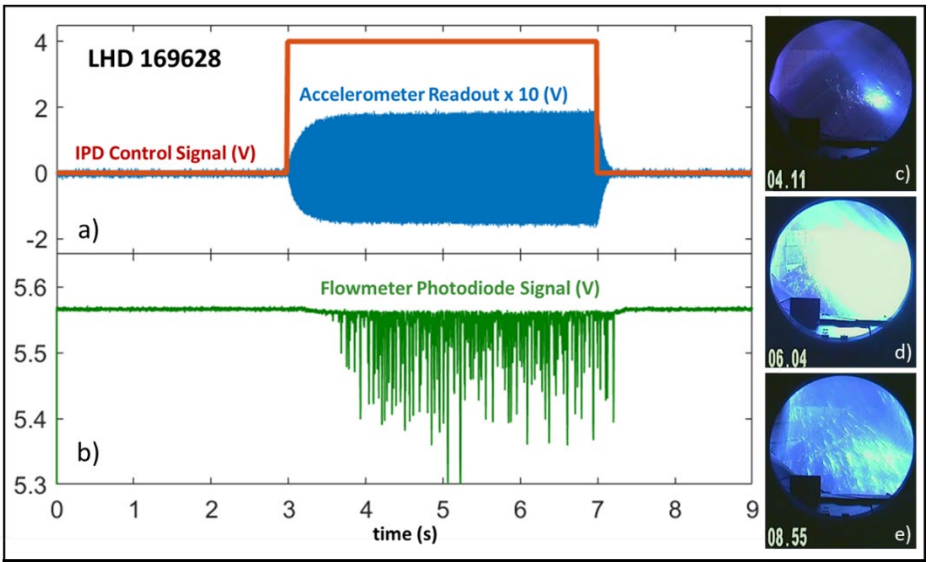

Figure 2 : IPD signals from the LHD experiment 169628. Engagement of the IPD control signal, as shown in panel a), starts the IPD. Positive operation is seen in the accelerometer readout with characteristic ramp up and decay time. Powder dropped from the IPD is monitored through negative deviations of the flowmeter photodiode signal in panel b) and direct camera observation as seen in panels c), d) & e) which show the beginning, middle, and end of the injection respectively. The delay from initiation of the control signal to first appearance of powder in LHD is due to gravitational transit time from IPD to plasma edge.

For these experiments two of the four IPD reservoirs were filled with 150 micron boron (B) and 60 micron boron nitride (BN) powders respectively. Powders were then injected at various times and throughput levels into the stationary portion of LHD discharges. Confirmation of successful injection was provided by a visible camera aimed at the injection site as shown in panels c - e of figure 2. The camera is mounted on an adjacent port to the IPD in the upper portion of section 2.5 with the field of view illustrated by the blue cone in panel a) of figure 1. In addition, entrainment of impurities into the plasmas is confirmed by spectroscopic measurement.

2.2 LHD

The distinct magnetic geometry of the Large Helical Device (LHD)[21] is formed by a 10 period externally wound continuous helical superconducting coils and a complementary superconducting poloidal coil set. These allow generation of an intrinsically stable helically twisted plasma which mitigates the need for

substantial internal plasma current as is nominally found in tokamak type devices. The double null structure of the magnetic field can be seen in the field line plot shown in panel a) of figure 1. The four legs of the magnetic field connect the graphite divertor plates to a thick ergodic region generated through the superposition of a magnetic island chain enclosing the main plasma volume.

2.2.1 LHD Standard Wall Conditioning

The interior surfaces of LHD are primarily comprised of 730 m^2 of stainless steel forming the primary vacuum vessel with a 50 m^2 helical series of graphite divertor plates comprising the principal plasma contact surfaces. Over the course of normal plasma operations, a co-deposition layer of carbon mixed with components of stainless steel is then observed[22] to coat the main vessel walls. These vessel components provide intrinsic impurity sources for the carbon, oxygen and iron spectroscopic signatures observed in standard LHD discharges.

To condition the plasma facing surfaces of LHD, standard boronization is applied by striking a glow discharge into a gaseous mixture of helium and a 10% diborane (B_2H_6) dopant[23, 24] before the start of an experimental campaign. Three toroidally distributed nozzles are used to introduce the diborane gas into the vessel which is then dissociated into constituent atoms by the helium glow discharge. The majority of the boron plates out on to the walls while the hydrogen is evacuated from the vessel. A series of 6 diborane detectors as well as a specialized catalyzer and dedicated filter unit are used to ensure a non-toxic gas exhaust. After the mixture gas introduction is stopped, the He glow discharge is continued typically for an additional 3 hours to reduce residual hydrogen in the deposited boron layer.

2.3 IPD Injection modelling

The unique magnetic geometry of LHD means that rather than being directly introduced into the crown of a tokamak type discharge on the Low Field Side as on ASDEX[18] or High Field Side as on EAST[14] the gravitationally injected powder must first cross a section of the upper divertor leg to reach the confined region. During this transit, the main additional force acting on the falling powder is an ion flow drag proportional to plasma density[25]. To ensure that the powder parameters chosen for these experiments would result in successful entrainment into the confined plasma an initial evaluation of the powder injection trajectories was predicted by coupled simulation using the EMC3-EIRENE and DUSTT[26] codes. This provides a better understanding of the processes which occur during powder injection and leads to conditions supportive of the real time boronization efforts which in turn guide the choices for plasma parameters utilized in the initial LHD-IPD experiments[27]. The 3D Monte Carlo code EMC3 which models edge and scrape off layer plasma transport is supplemented with the EIRENE model of neutral dynamics. For these simulations the experimental profiles of electron density as well as electron and ion temperatures are provided by Thomson scattering and charge exchange spectroscopy. These profiles are then matched to the diffusion and thermal conductivity coefficients for the main plasma ions within the simulations. Once a self-consistent solution has been reached this parameter set is used as the background against which DUSTT simulations of 3D particle trajectories are computed. For these simulations 150 micron boron powder particles are created with an initial downward velocity of 5 m/s at

a location just above the upper divertor leg. This corresponds to the conditions of an estimated free falling powder particle immediately before interacting with the plasma. While these calculations showed substantial deflection of the incident powder by ion flow within the upper divertor legs of LHD, the positioning of the IPD on the radially innermost port provides sufficient margin to ensure reasonable powder assimilation.

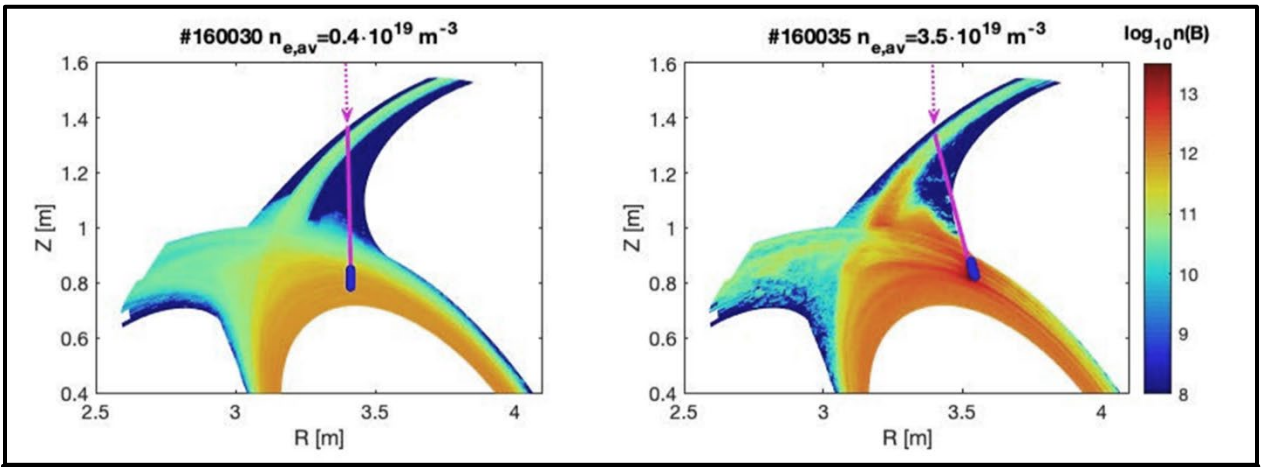

Figure 3: Simulated boron powder injection trajectories into low density and high density plasmas. The coupled IPD injection simulations are provided by the EMC3-EIRENE and DUSTT codes. B powder trajectories are shown by the vertical magenta line while the blue dots indicate the positions where the neutral boron atoms are provided to the simulation by the evaporation of the plasma heat load. These injection trajectories are superimposed over the EMC3-EIRENE generated B ion distributions as summed over all ionization states.

The left hand image shows powder particle trajectories for the low density cases (n_e = 0.4x10^{19} m^{-3}) with minimal deflection being shown to the injection trajectory as the powder transits the divertor leg and enters the confined plasma. The blue marker indicates the approximate location of full ablation with the color coding representative of the boron ion distribution as summed over all of the ionization states. This is contrasted with the high density case where the powder trajectory is significantly deflected by the entrained ion drag force within the divertor leg plasma flow. While this does not contribute significantly to the particle ablation, the deflection results in a more peripheral location for the ion source term. As a result there is greater toroidal uniformity of the powder distribution in the low density case as the deeper penetration allows greater homogenization. This is consistent with the findings of the predictive investigation[28] which was performed before the injection series and also matches the more limited impact of the powder injections observed in the higher density cases.

3. Experiment

For this series of experiments we explore the prompt and long term effects of power injection in standard pulse (< 8s), long pulse (~40s) and extreme long pulse (>100s) discharges in turn. Injections with a multitude of heating sources are explored as well as injection into H, D, and He fill gasses utilizing both B and BN injection species. Powder injection discharges were interspersed with control discharges to

determine any cumulative modification of the recycling rate of the vessel. In addition intrinsic impurity concentrations were monitored for gettering effects attributable to the newly deposited boron layers. Injection of powder was observed to successfully penetrate into the main plasma volume with these injections briefly increasing plasma density as well as total radiated power.

3.1 Standard Length Discharges

Typical time evolutions of the plasmas parameters for standard length plasmas can be seen in figure 4. For the discharges shown, the solid lines (169616 and 169621) were reference discharges while the dashed lines (169618 and 169623) indicate powder injected plasmas. Auxiliary heating for all discharges is primarily provided by the combined contributions of neutral beams 1-3, which are tangentially injected, with electron cyclotron heating applied at the beginning of the discharge to provide an impetus for volume breakdown. Diagnostic pulses from NBI 4 & 5, which are perpendicularly injected are employed to recover charge exchange information which is in turn utilized to determine the ion temperature. Throughout the remaining panels of the figure we compare the control discharges with powder injection discharges for pre-programmed plasma densities of $2x10^{19}$ m^{-3} and $4x10^{19}$ m^{-3}. While no variation is observed in the feedback controlled plasma densities both with and without powder injection, as is shown in the third

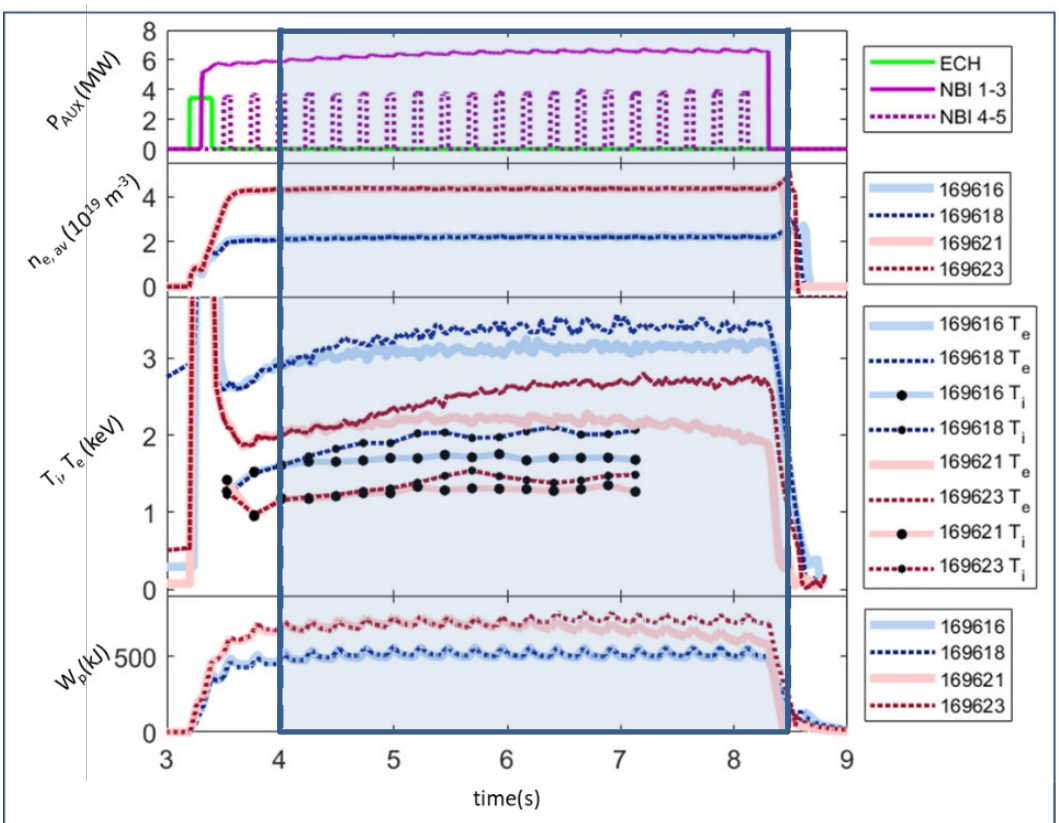

Figure 4 : Time traces for control and IPD injection plasmas. Heating scheme for the standard pulse length is shown in the top panel with the lower and upper feedback controlled densities in the second panel. In the T_e and T_i panel(3rd) as well as the 4th panel showing stored energy traces, the solid lines represent the control discharges without powder injection(169616 & 169621) while the dashed lines correspond to plasma evolutions which include powder injection(169618 & 169623). The shaded box denotes the period of powder injection.

panel, there are elevations to both the electron and ion temperatures coincident with powder injection. These enhancements to plasma performance are fully detailed in Ref [19] which notes that these periods align with a decrease in turbulent fluctuations and a corresponding reduction in anomalous transport. The radial profile shaping denoted as the nascent cause of this turbulence suppression appears to be similar to that observed both during carbon pellet injection experiments on LHD[29-31] as well as on Wendelstein 7-X during periods of enhanced confinement [17, 32-34]. As these phenomena are better described elsewhere we merely note that while not anticipated during these experiments, these results are not without precedent.

Confirmation of positive injection and plasma entrainment is obtained by observation of spectroscopic boron signatures[35] coincident with the period of injection. Figure 5 shows the time evolution of the Boron II signal at 136.25 nm in panel a) and the Boron V signal at 4.86 nm in panel b). As can be seen, the background plasma density ($2x10^{19}$ m^{-3} for LHD 169618 (blue) and $4x10^{19}$ m^{-3} for LHD 169623(red)) has little effect on the boron signal level for both BII and BV signatures while the increase in IPD voltage for LHD 169626 understandably leads to a greater injection quantity and thus a greater signal level. However while the boron V signal plateaus at a level mildly elevated over the lower injection rates, the boron II signal line continues to increase throughout the discharge.

While detailed ion transport modelling for these scenarios has yet to be undertaken and as such a comprehensive understanding of the mechanisms of powder assimilation are still in the nascent stage we can make some basic observations which could help to explain this phenomenon. Examining panels c) and d) which show fitted electron density and temperature profiles at t = 7s from Thomson scattering measurements, we see that there are substantial differences between the baseline discharge LHD 169616 and the pair of powder injection discharges LHD 169618 (IPD @ 6V) and LHD 169626 (IPD @ 7V). The steepening of the edge density profiles and elevation of the core temperatures are consistent with those observed during boron carbide pulse injection in W7-X[17] and are further examined in [19]. For this particular discussion we note that there do not appear to be any substantial differences between the profiles obtained during the pair of B injection discharges which could help explain, through a change in transport regime, the elevated boron-II levels in the higher injection discharge. What could explain this difference is an observed ramping of the boron injection level as shown in flowmeter readout for the IPD in panel e). During changes of settings to the IPD there is sometimes a lag which is observed between the requesting of a powder output level and the full realization of this level. In addition the elevated level of excitation is more likely to break up agglomerated boron chunks which might not normally flow through the IPD channel. These can be indicated by larger point like boron clumps as seen by the increasing level of negative spikes. While this offers a plausible explains the elevated boron-II levels, it does not provide a corresponding clarification for the plateau of the boron-V signal. However, if there is significant impurity screening in the ergodic layer due to high edge collisionality as suggested in [36-38] it could explain the buildup of lower ionization state impurity ions in the edge region. The screening could also explain why the increased injection level only results in a mild enhancement of the resulting boron V signal.

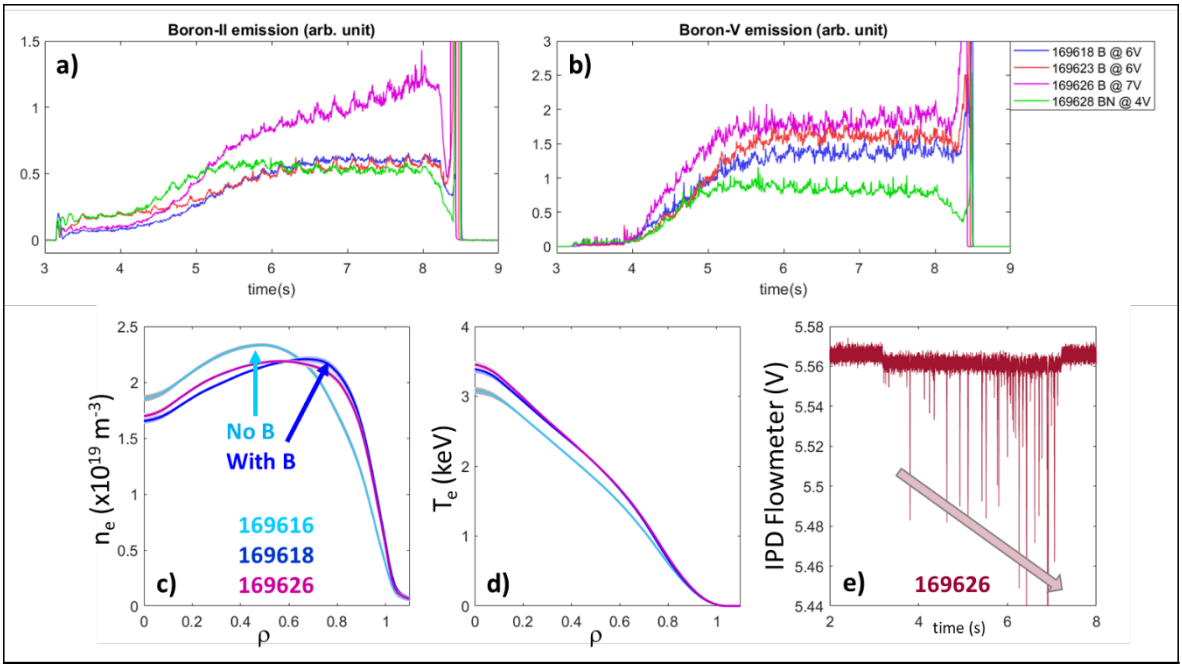

Figure 5 : Plasma behavior in response to boron and boron nitride particulate injection. Panels a) and b) confirm entrainment of boron species coincident with powder injection through spectroscopic measurement while panels c) and d) display the changes in electron density and temperature profiles with corresponding error bands from Thomson scattering measurements. Panel e) is the signal recorded from the IPD flowmeter for LHD 169626 showing an increasing level of injection through the plasma evolution. The arrow has been added to guide the eye.

Returning to panel b of figure 5 we also note a reduced boron V signal level during Boron Nitride injections in LHD 169628. The utilization of Boron Nitride in initial IPD experiments was due to the physical properties of the medium[13]. As a recognized lubricant and a compound often found within fusion research devices it was introduced in some of the first IPD experiments on ASDEX-Upgrade due to the ability to maintain fine control over the injection quantity. The unexpected beneficial result of these injections was an observed increase in confinement on the full metal wall machine in a manner similar to that of nitrogen gas puffing[18]. Experiments were attempted on LHD to see if there was a similar effect. In these experiments we note that while boron-II level asymptotes to a similar level as that seen in the corresponding pure boron injection, the B-V level is nearly a factor of 2 lower. We postulate that this may be the result of a decreased entrainment of the smaller BN particulates(60 microns for BN vs 150 microns for pure B). As shown in the injection modelling[26] the smaller injection media are more likely to be redirected by the divertor plasma flow during the initial injection process. The BN, being of smaller size, is deflected by a more substantial amount leading to a reduced fraction of the material entering the fully confined region and thus reaching an elevated ionization state.

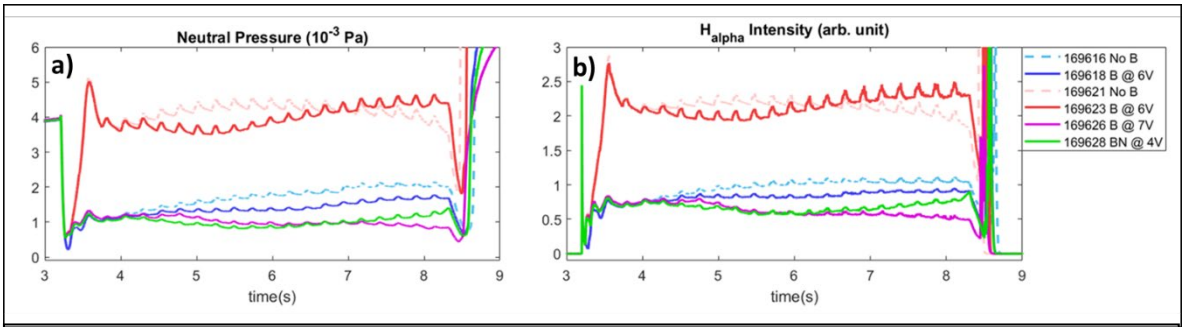

Figure 6 : Changes in neutral particle pressure and Hα intensity. These measurements serve as a proxy for a direct wall recycling measurement. For both high and low density measurements the control discharges are denoted by the lighter broken lines.

3.1.1 Evidence of prompt changes to recycling

The application of boron powder into the plasmas has been shown to contribute to thin layer formation over the plasma facing components[12]. This layer is then thought to be responsible for the reduction in recycling in a manner similar to that observed during standard glow discharge boronizations[39, 40]. The deposited boron layer shows evidence of oxygen gettering and the chemical formation of compounds such as BO, B_2O, B_2O_2, and B_2O_3[41]. This in turn leads to the demonstrated ability of a mixed boron/carbon surface or BCO-x film to retain hydrogen isotopes more effectively as compared to a pure carbon surface.[42].

The prompt effect of powder injection on the wall conditioning can be observed by examining the evolution of the neutral pressure and Hα measurement over the course of the discharge. These quantities, interpreted as indicators of improved recycling control, are shown in panels a) and b) of figure 6 for the series of discharges. For the lower density discharges, a reduction of both the Hα signal as well as the neutral pressure is observed after powder injection with stronger reductions observed for the larger powder injection quantities. As the boron containing compounds are injected, one might expect the electron density to increase due to the introduction of additional material, however if this were the case a corresponding reduction of fueling would also be observed. Examining the top panel of figure 7 we observe that there is actually an increase in the fueling rate for the B containing discharge. As such it seems more likely that the reduction in neutral pressure and Hα measurement observed in this discharge is due to an enhancement of the wall pumping by the newly deposited B layer leading to a decrease in the electron density. For feedback controlled discharges such as these, this results in an increased level of fueling needed to maintain the density setpoint. The competing effects of the injected material and increased pumping can be seen in the lower panel of figure 7 where the gas puffing level for the plasmas with elevated B injection rate (169626) is similar to the control discharge despite strong reductions in the neutral pressure and Hα seen in figure 6. This is believed to be the result of the additive electron burden introduced by the B powder counteracting the increased wall pumping resultant from the powder injection.

These contraindicating behaviors are also observed in a very specific manner during the higher density discharges. Examining the powder injection discharge LHD 169623 when compared to its respective control discharge LHD 169621 we see a reduction in the observed neutral gas and Hα signals from 4s to approximately 6.5s indicating a reduction in recycling as was seen with the other experiments. As this appears to reverse after t=7s, it could possibly give one the indication of a sharp increase in recycling. However, we note that during the high density control discharge the gas puff level decreases as the shot progresses, as shown in the middle panel of figure 7. This indicates a saturation of the walls and the beginnings of a loss of density control. Because of the reduction in fueling rate the neutral pressure and Hα levels start to tail off sharply after t = 7s. In contrast, the increased wall capacity from the newly deposited boron layer in discharge 169623 allows the gas puffing rate to remain high during the latter stages of plasma development which keeps the neutral pressure and Hα levels elevated when compared to the control discharge. Thus it is not a reduction in the efficiency of the coating layer which is indicated by the uptick in neutral pressure and Hα, but rather a confirmation of the positive effects of particulate conditioning as evidenced by extended period of density control. Finally, the transition from B to BN as the injection species does not appear to inhibit the ability of the injected boron to reduce recycling or Hα. The primary difference noted is an increase in the overall plasma radiated power as is to be expected with the injection of the concomitant nitrogen.

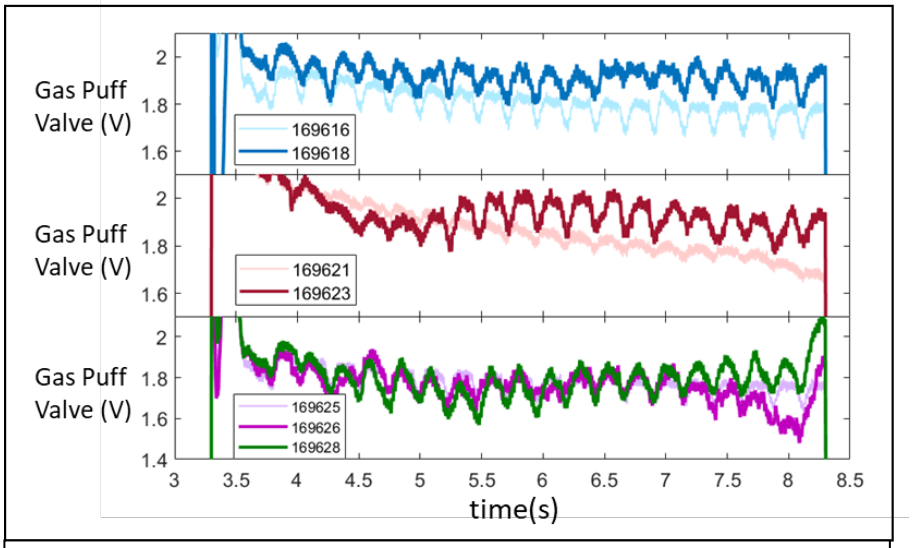

Figure 7 : Gas puff introduction into conditioning and control plasmas. Lighter colors represent discharges without particulate injection (Discharges 169616, 169621 and 169625) while the darker traces correspond to powder injection discharges(169616, 169623, 169626 and 169628).

3.1.2 Powder injection effects on intrinsic impurity levels

An additional measure of the ability of the injected material to condition the plasma is through the flushing of intrinsic impurities. It has been observed in several other devices that the introduction of low z materials through powder or granule injection leads to a reduction in levels of intrinsic discharge impurities[43]. Whether this is due to a reduction of the source term by application of a boron coating, or as a flushing of the present impurity through a neoclassical effect, the result is consistent across experiments. For the recent experiments on LHD we are monitoring the Carbon(C-IV), Oxygen (O-VI) and Iron(Fe-XVI) line intensity evolutions over the course of the discharge.

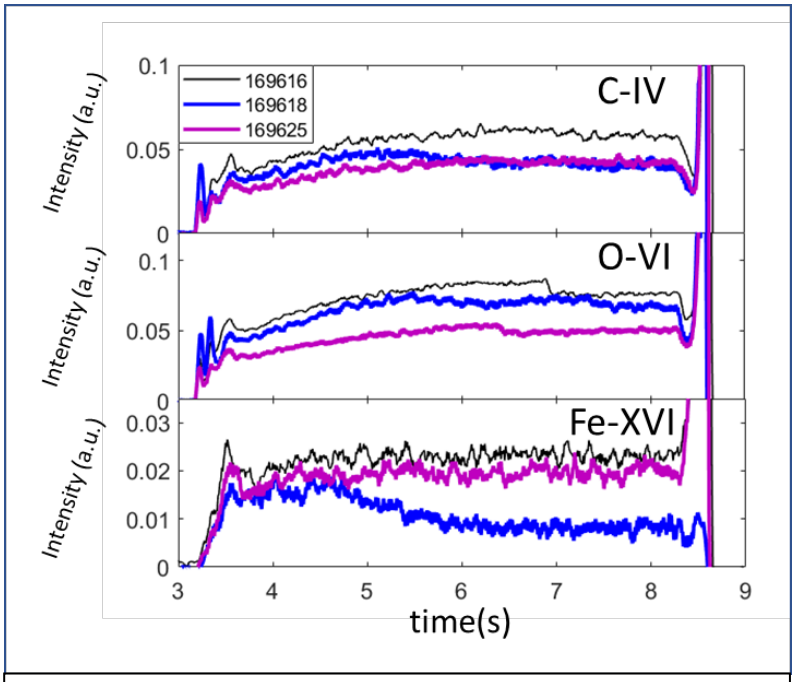

Figure 8 : Impurity evolution with powder injection. Differences between the initial control discharge LHD 169616 without powder and a discharge with powder injection LHD 169618 are shown as well as a second control discharge, LHD 169625 taken after several injection discharges.

As can be seen in figure 8, the application of powder within LHD 169618 leads to a reduction of the normalized spectral intensity of the monitored impurities over the course of the discharge. During the periods of B injection there is a substantial reduction in the iron signature (bottom panel) as well as a reduction in the carbon signatures(top panel). Oxygen levels(middle panel), while still reduced do not appear to be flushed as significantly. Long term effects of powder injection, attributable to cumulative conditioning effects can be observed by variation in signal levels recorded during control discharges at the beginning(169616) and end(169625) of the injection series. For these discharges the effect is most notable in the intrinsic carbon and oxygen impurities which are both reduced by 25%-35%. We suggest that this is further evidence of the deposition of a boron layer in the plasma facing surfaces and the

resulting absorption of carbon and oxygen impurities as provided by this layer. The Fe impurity contribution inherent in the discharges is provided by sputtering from the LHD stainless steel shell. So while the presence of B in the discharge can be expected to flush the Fe from the plasma as seen with the other IPD and IGI experiments[12-14,18] the limited contact between the plasma and the SS shell suggests minimal generation of an appreciable B coating on this surface during periods of moderate IPD application. Thus given this limited coating, it is not surprising to see that the spectroscopic signature of Fe does not decrease significantly over the course of the conditioning discharges.

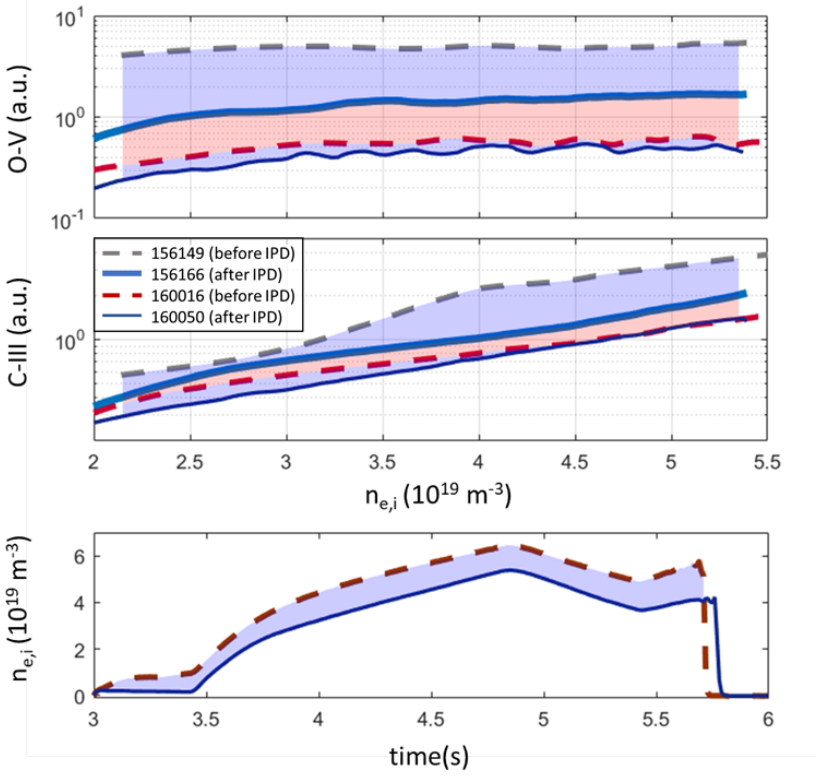

Figure 9 : Long term effects of conditioning injections on baseline discharge impurity levels. The top panels display the change in O-V and C-III impurity signatures as a function of the line integrated densities during control discharges. The plots show the evolution of impurity levels which occur between the beginning of the experimental series and the initial boron injection, after a standard B_2H_6 boronization, and then again after further boron particulate injections. The lower panel shows the variation in density evolutions for identical fueling programs before and after the injection of boron particulates.

3.1.3 Cumulative effects of powder injection on impurities

The results of conditioning injections on the intensity of the O-V and C-III impurity lines are shown in figure 9. The signals are plotted vs the line averaged plasma density for a set of density ramping control discharges taken at various points during the experimental series. These experiments were undertaken in the Rax = 3.6 m configuration with the first discharge of the series (156149, denoted by the grey dotted line) occurring after a vessel vent and before a subsequent standard boronization. The presence of a recent vent just prior to this control discharge explains the relatively high oxygen concentration. After a series of IPD dropper experiments whereby approximately 2g of boron is deposited into the vessel the oxygen content can be seen to have dropped by over a factor of 2 as shown by the blue solid line depicting signatures recorded during discharge 156166. The respective colored blue area is used to help illustrate the reduction observed between the initiation and completion of Impurity Powder Dropper operations. Between the first and second series of IPD experiments a standard B_2H_6 gaseous boronization was applied to the LHD vessel depositing an additional 37g of boron over the interior surfaces. This is responsible for the new reduced oxygen and carbon concentrations as shown by the orange dashed line and red shaded area. The injection of an additional 1g of boron by the IPD during the period between discharges 160016 and 160050 was successful in further reducing the oxygen impurity level slightly, but as expected, the effect is not as evident in a newly boronized vacuum vessel with already exemplary wall conditions. These results are consistent with the gettering of the oxygen within the vessel by the newly deposited boron layer. Additional evidence of a wall conditioning effect is demonstrated in the lower panel of figure 9. In this figure we are again comparing the performance of the control discharges before and after application of boron powder, specifically the changes observed in line averaged electron density in response to a constant fueling envelope. As shown, the evolution of the density after injections of B and BN injections totaling approximately 1g, as indicated by the solid line, is 18% lower than the density response to an identical gas puff profile applied before the powder injection as represented by the dotted line. We assert that this clear indication of a change in the recycling rate is most likely due to the deposition of a thin B film on the relevant PFCs and the interaction of the fill gas with that film.

3.2 Long Pulse Discharges and dust assimilation

To further investigate the effects of powder introduction on wall conditioning and plasma performance a series of injections were also introduced into 40-second long plasmas. The set consisted of electron cyclotron heated hydrogen and helium plasmas into which powder is injected for up to 15s. These extended powder introduction phases allow initial observations of true real-time wall conditioning. The fuel gas is feedback controlled until t = 20s for He or t = 15s for H after which the gas injection is stopped for the remainder of the discharge evolution. The entry of the powder into the plasma and its subsequent rapid assimilation is evidenced by the sharp increase of the spectroscopic boron-V signal which quickly reaches a quasi-static elevated level, with spike-like deviations due to the introduction of aggregate clumps of powder. The rapid ablation and ionization of the injected material also leads to a rapid increase in the electron density with respect to the reference discharges similar to what was observed in the shorter discharges as described in [27]. In panel a) of figure 10 a shorter boron pulse was introduced to allow observation of the long term effects of powder injection on the density evolution. As shown, the overall density level is observed to sharply decrease and remain at this lower level throughout the remainder of the discharge.

The reduction of density seen in the top panels of figure 10 is interpreted as a corresponding reduction in the recycling level due to gettering of fuel gas by the injected boron which is being expelled from the plasma and plating out on the walls. This behavior of the boron impurities is supported by the observation that the boron signal level plateaus despite continuing injection for multiple seconds. The fact that we are not seeing a ramping boron signal means that it is being exhausted and driven from the plasma. In addition, the observation that the electron density remains lower than the reference level even to periods long after the powder injection has completed again indicates the ability of the exhausted boron particulates to affect the recycling through co-deposition of the main ions onto the plasma facing components and then continue to do so in a manner consistent with the deposition of a thin gettering layer of material reducing the influx of neutral gas from the wall.

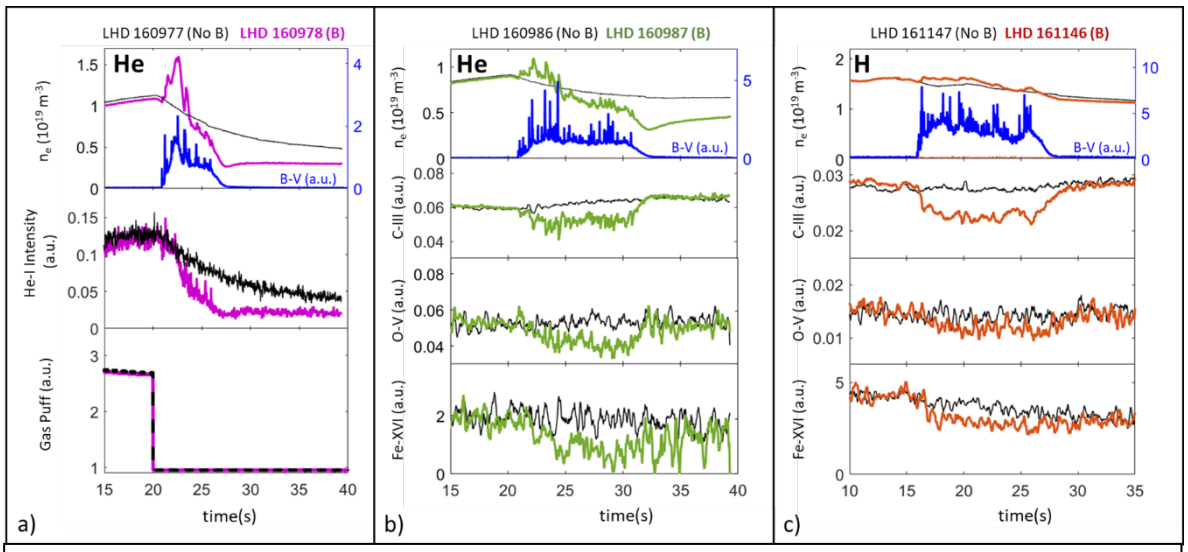

Figure 10 : Response of plasma evolution to extended powder injection in long pulse discharges. Each panel shows the comparison between an IPD injection discharge in color and the corresponding control plasma in black.

An additional observed effect, common to both the injections short and long pulse injections into LHD is the ability of injected materials to flush higher Z impurities. As shown in the lower three plots of panels b) and c) of figure 10, the introduction of B containing powders leads to an observed reduction of C-III, O-V and Fe-XVI during the period of the dropper activation. Here the spectroscopic signals of the control plasmas without IPD injection, normalized to the electron density, are compared to the signals resulting from plasmas which include IPD injections. Again we note a stronger effect in the low density He discharge than was observed in the high density H discharge, consistent with the greater assimilation of material into the plasma. However in all cases we note that the impurity level quickly returns to match the control plasma level once the active portion of the dropper injection is stopped. This may indicate that the introduction of the boron powder to the plasma was producing a change in transport resulting in impurity

flushing, rather than a change in the impurity source as a result of particulate wall conditioning. This does not mean that there were no long term conditioning effects, as evidenced by the density reductions, simply that the quantity of injected material was insufficient to provide demonstrable proof of longer term conditioning within the single discharge.

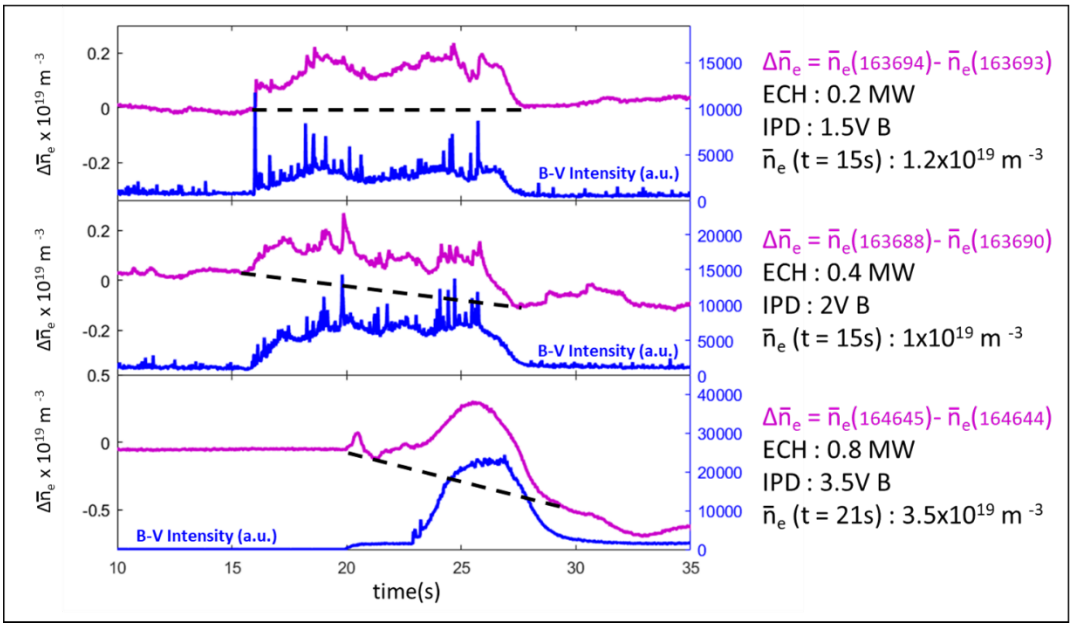

Figure 11 : Change in density during deuterium long pulse discharges. The three above panels show the difference in density evolution between the control discharge and the IPD injection discharge for three distinct auxiliary heating levels. The black dotted line is overlaid on the density trace to illustrate the change in baseline level evolution over the period of injection.

In addition to injections into H and He long pulse discharges, a series of B powder injection was performed into deuterium plasmas at a range of densities and input powers. These 40s plasmas were injected with either B from 15-25s or BN from 20-30s to further explore the effects of extended injections. The three panels of figure 11 explore the evolution of the change in density over the course of, and after the series of injections. All discharges are supported by 2.0 MW of ICH heating along with variable steps of ECH power. At the reduced input power (ECH = 200kW) the energy losses due to powder ionization and assimilation can be substantial enough to result in a discharge collapse, as such the powder injection rate must be limited. Subtracting the density of the B injection plasma from the control plasma we see that the increase in density closely mirrors the behavior of the spectroscopic boron signal with the increase in density being completed as the B powder injection is stopped. Thus the final density observed after the completion of the injection is similar to the density level observed prior to the injection. This would indicate that at this input power level and powder injection level there was not substantial wall pumping.

When the ECH auxiliary heating power is increased from 200kW to 400kW the elevated heating level permits a greater powder introduction rate and given this we now observe the overlay of a pair of competing behaviors similar to what was seen during the shorter discharges. As can be seen in the second

panel while the overall system density does increase over the control plasma as a result of the B injection, if we follow the course of the plasma evolution throughout the drop period we find that this increase in density is overlaid on a negative sloping discharge baseline, and that once the injection is concluded the plasma now evolves from this new lowered baseline throughout the remainder of the discharge. Thus the powder dropper is able to demonstrate a real time density control effect on long pulse plasmas.

This effect is further confirmed in the third panel of the figure set where an elevated ECH level of 800 kW, a higher baseline density of $3.5x10^{19}$ m^{-3} and a B introduction voltage of 3.5V lead to an even steeper reduction of the overall plasma density. Here the powder was introduced from 22s to 27s and demonstrates an even stronger reduction of the baseline density with the effect continuing even after the powder cessation. This could indicate not just density control but also the beginnings of a conditioning layer formation.

We conclude this study by observing the effects of B powder injection on extreme long pulse He plasmas as shown in figure 12. For these discharges powder was injected starting at 110s, when the original discharge began to exhibit loss of density control, until the conclusion of the plasma at t = 168s. As the recycling is larger than unity the gas injection system is shuttered and the density evolution is uncontrolled. During the powder injection discharge, density rises as new material is absorbed, but soon drops back below the feedback setpoint due to the reduction in nominal density caused by the now enhanced wall pumping. It is not until an additional 10s burst of fuel gas that the other discharge begins to exhibit a similar loss of density control. In the B injection discharge there are coincident spikes visible in the plasma density, iron impurity signature and radiated power at t = 143s just as the density starts to ramp leading to the supposition that a piece of wall material may have entered the discharge and possibly destabilized the plasma, an event from which the discharge was unable to completely recover.

Normalizing the spectroscopic impurity signatures to the plasma density we observe that there is a continued reduction in oxygen impurities as a result of the boron powder injection. This is understandable as a result of the chemical affinity of B and O. There is also a initial slight reduction in the overall iron intensity, although the full evolutions return to a concurrent state by the end of the discharge. Helium and carbon signatures are also observed to initially decrease mildly, however this trend is reversed during the period of additional gas fill. Following the evolution through to the end of the discharge we note that the carbon signature again trends downward, while the helium evolution is essentially the same as the control discharge.

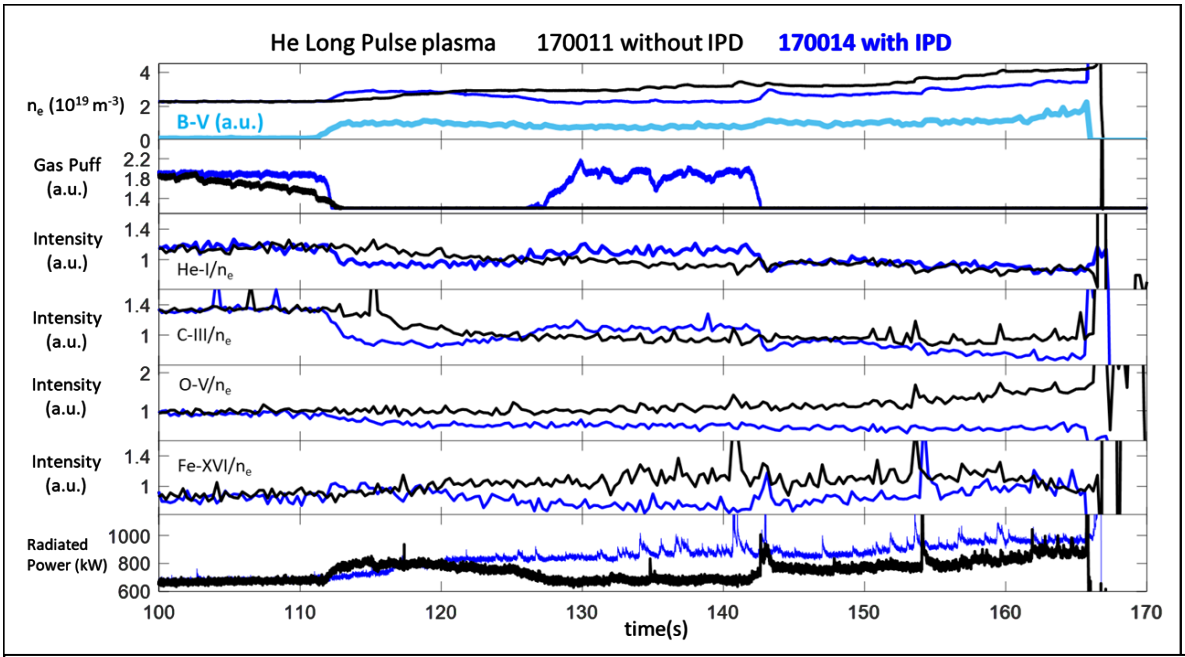

Figure 12: Evolution of plasma parameters in extreme long pulse He discharge. The black traces throughout the panels show evolution of a plasma without IPD injection while the blue traces correspond to plasma responses to IPD injection. The light blue trace in the top panel is the spectroscopic boron-V signal and denotes the period of injection. Spectroscopic traces are normalized to the evolving averaged plasma density and scaled by unitizing the corresponding value of the control discharge at the midpoint of the time period of interest.

The reduction in overall density observed during the initial powder injection is of interest given the helium fill gas utilized for this particular set of discharges. We note here that when the H or D fill gas is captured by the deposited layer it is reasonable to assume that a portion of this is due to chemical bonding due to the natural affinity of the borate series of compounds. However such chemical formations do not occur with a noble fill gas such as He and thus some other avenues of aggregation must be explored. Previous LHD postmortem analysis has shown a first wall mixed material depositional coating comprised predominantly of carbon and trace amounts of iron[22]. This amorphous nature of this layer appears to act as an attractive trapping site for helium during long pulse discharges[44]. Thus it is possible that an enhancement to this layer by the additional boron coating could reasonably lead to an additional adhesion of helium to the first wall. However, this remains an open research question with future experiments proposed to better determine the true underlying mechanism.

3.3 First wall observation of boron coating layer buildup

The evidence presented so far, while all completely consistent with the evolution of a boron layer formation can not be said to be completely conclusive without direct observation. To assess coating effectiveness a 316 stainless steel sample specimen was inserted from a lower vessel port to be flush with the first wall position in section 4.5 lower port located 72 degrees toroidally apart from the point of IPD injection. A poloidal cross-section of the LHD vacuum vessel can be drawn as a circle with diameter of 3.2m with contours removed for the helical coil grooves. For these experiments, the stainless steel samples were located at the first wall relevant position as shown in the drawing on the left hand side of figure 13. A single specimen was exposed to the plasma for a subset of the duration of the IPD experiments on December 3rd and 6th 2019 with the total boron quantity dropped during these experiments estimated at about 800 mg. Another material sample was inserted prior to a standard B_2H_6 boronization on LHD to provide a comparison. An analysis of the coatings on these samples was performed ex-situ using Glow Discharge Optical Emission Spectroscopy [45]. With this method an argon glow discharge is utilized to sputter micro-layers from the sample allowing a record of the composite depth profiles found upon these samples to be discerned. This comparison is displayed in the graphs on the right hand side of figure 13.

For the samples shown here the depth of the layer is determined by sputtering time needed to remove the coating. Overall layer depth is determined by shine through of the substrate, in this case Fe from the steel, with longer times indicating thicker coatings. The indications of a boron coating on this first wall-equivalent section is noteworthy as the injections were undertaken during operation of the LHD magnetic fields and as such preferential transport to the divertors is expected. Evidence of material transport to additional first wall surfaces, either through direct deposition or through a multi-step evaporation and redeposition process is supportive of a powder injector type device being able to provide some aspect of first wall maintenance without the need to curtail standard operational scenarios.

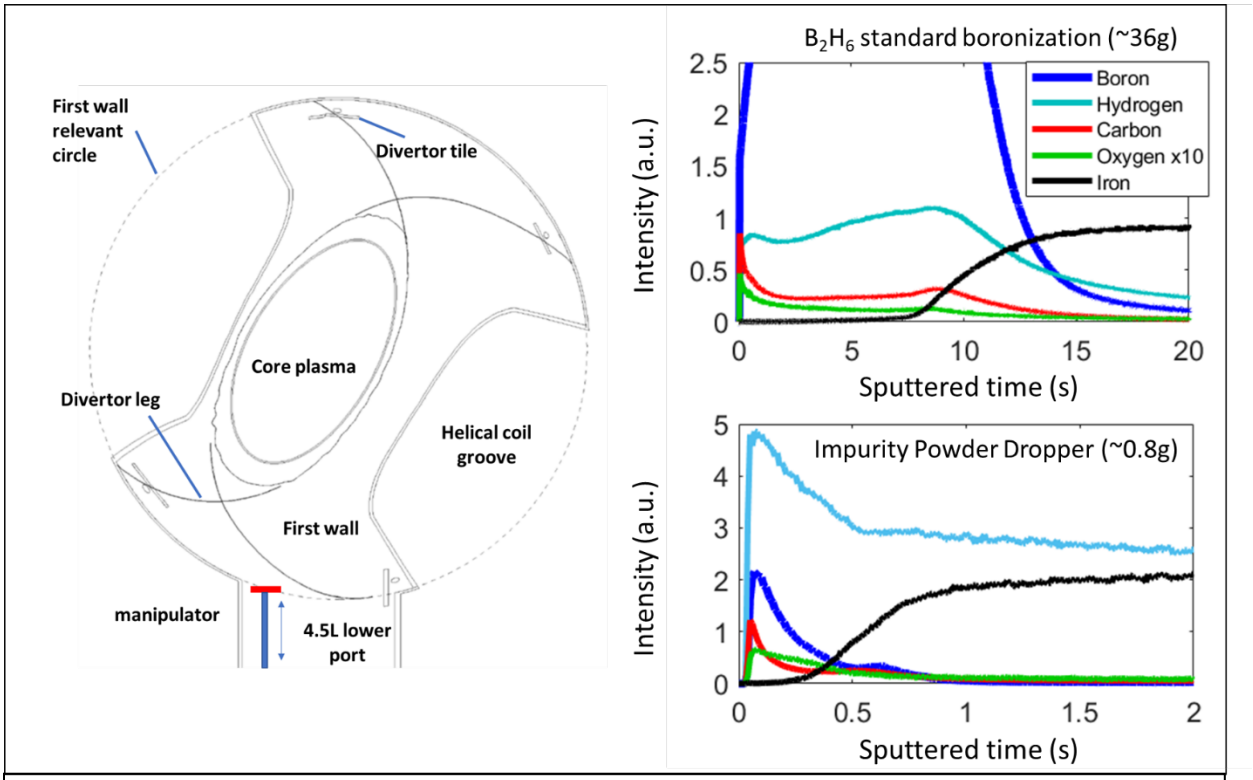

Figure 13 : Diagram of the manipulator location (left) and optical emission spectroscopy readout for specimen exposed to standard boronization and to impurity powder dropper coating(right). Note that as the standard boronization deposits substantially more material it results in a much thicker coating and the axes have been adjusted to reflect this.

5. SUMMARY

We report here a comprehensive study of recycling and wall conditioning response to powder injection over multiple discharge lengths, multiple heating methods, plasma densities and fill gasses. The demonstration of robust conditioning effects over all the parameters demonstrates that the utilization of particulate based real time wall conditioning is a versatile tool for modifying and maintaining plasma wall interactions. Upon first inspection these results appear to be compatible with the requirements of a real time boronization system in a steady state device, although further research is suggested as these results need to be confirmed for higher density plasmas with greater heating power.

The injection of boron and boron nitride powders into LHD plasmas has been observed to have beneficial effects on the plasma material interface both in real time and cumulatively over a series of discharges. These benefits are reported for both H and He plasmas, with the stronger results in the latter believe to be more dependent upon overall plasma density than a species specific effect. Coupled simulations with the EMC3-EIRENE and DUSTT codes confirm observations that with the present powder inventory and injection location the low-density plasmas are more efficient at full material assimilation and thus results

in more uniform distribution of B atoms at the plasma facing components. As such these scenarios might be more favorable for future conditioning type discharges with the IPD as the B impurity ions are continually flushed from the discharge providing an effective coating mechanism.

The present limitation of powder deflection by the divertor flow can be surmounted by the utilization of larger grain sizes within the applied powder as long as the volumetric flow rate from the IPD has been compensated to maintain mass throughput. This can also allow conditioning injections to be undertaken in higher density discharges where smaller particles might otherwise be fully deflected. Operations in this regime may be more relevant for future reactor scale operations. Such experiments have been undertaken and will be the focus of future analysis.

In addition the observed changes to the plasma density and temperature as a result of injections into extended duration plasmas opens up the possibility of utilizing the IPD as an additional plasma control tool for research purposes. Testing of these powder dropper feeders for extended periods in extreme long pulse LHD discharges has also determined that the length of the injection is limited only by the available quantity of powder. In addition the ability to generate pulses of variable length and intensity multiple times within a discharge provides a controllability to the application of particulate material which would be necessary if one were to utilize the dropper in a feedback control manner. This is especially noteworthy as the world fusion program begins to explore the complex physics of long pulse discharges. A delivery device such as the IPD could be envisioned as a method for intra-shot conditioning to allow extreme long pulse discharges. Such conditioning would be required due to deterioration of low Z coatings on metal walls and the resultant increase in high Z sputtering.

6. ACKNOWLEDGEMENTS

The authors would like to thank full LHD team for their dedicated support and assistance especially considering the challenging remote collaboration requirements. This work was conducted within the framework of the NIFS/PPPL International Collaboration, and it is supported by the LHD project budget NIFS19ULFF022 and by the U.S. Department Of Energy under Contract No. DE-AC02-09CH11466 with Princeton University. The LHD data can be accessed from the LHD data repository at https://www-lhd.nifs.ac.jp/pub/Repository_en.html.

7. REFERENCES

[1] K. Tobita *et al.*, "Conceptual design of Japan's fusion DEMO reactor (JADEMO) and superconducting coil issues" *J. Phys.: Conf. Ser* **1293** (2019) 012078

[2] G. Federici *et al.*, "DEMO design activity in Europe: Progress and updates" *Fusion Eng. and Design* **136** (2018) 729-741

[3] Y. Wan *et al.*, "Overview of the present progress and activities on the CFETR" *Nucl Fusion* **57** (2017) 102009

[4] K. Kim *et al*., "Design concept of K-DEMO for near-term implementation" *Nucl. Fusion* **55** (2015) 053027

[5] M. Tokitani *et al.*, "Microscopic modification of wall surface by glow discharge cleaning and its impact on vacuum properties of LHD" *Nucl. Fusion* **45** (2005) 1544

[6] S. Sereda *et al*., "Impact of boronizations on impurity sources and performance in Wendelstein 7-X" Nucl. Fusion **60** (2020) 086007

[7] X. Gao et al., "ICRF wall conditioning and plasma performance on EAST" 2009 J. Nucl. Mater. **390-391** 864-868

[8] K. Itami et al., "RF heated wall conditioning discharges in JT-60U" 2009 J. Nucl. Mater. **390-391** 983-987

[9] G. Giruzzi et al., 'Physics and operation oriented activities in preparation of the JT-60SA tokamak exploitation', 2017 Nucl. Fusion, **57** 085001

[10] T. Wauters et al., "Wall conditioning in fusion devices with superconducting coils" 2020 Plasma Phys. Control Fusion. **62** 034002

[11]H.W. Kugel *et al.*, "Lithium coatings on NSTX plasma facing components and its effects on boundary control, core plasma performance, and operation" *Fusion Eng. Des.* **85** (2010) 865-873

[12] A. Bortolon *et al.*, "Observations of wall conditioning by means of boron powder injection in DIII-D H-mode plasmas" *Nucl. Fusion* **60** (2020) 126010

[13] A.Bortolon *et al.*, "Real-time wall conditioning by controlled injection of boron and boron nitride powder in full tungsten wall ASDEX Upgrade" 2019 Nucl. Mater. Energy 19 384-389

[14] Z. Sun *et al*., "Suppression of edge localized modes with real-time boron injection using the tungsten divertor in EAST" *Nucl. Fusion* **61** 2021 014002

[15] E. P. Gilson *et al*., "Wall Conditioning and ELM Mitigation with Boron Nitride Powder Injection in KSTAR" *Nucl. Mater. Energy* **28** (2021) 101043

[16] R. Maingi *et al*., "The effect of progressively increasing lithium coatings on plasma discharge characteristics, transport, edge profiles and ELM stability in the National Spherical Torus Experiment" *Nucl. Fusion* **52** (2012) 083001

[17] R. Lunsford *et al*., "Characterization of injection and confinement improvement through impurity induced profile modifications on the Wendelstein 7-X stellarator" *Physics of Plasmas* **28** (2021) 082506

[18] R. Lunsford *et al*., “Active conditioning of ASDEX Upgrade tungsten plasma-facing components and discharge enhancement through boron and boron nitride particulate injection” *Nucl. Fusion* **59** (2019) 126034

[19] F. Nespoli *et al*., “"Observation of a reduced-turbulence regime with boron powder injection in a stellarator" *Nature Physics* 18, (2022) 350-356 [20] A. Nagy et al., “A multi-species powder dropper for magnetic fusion applications” Rev. Sci. Instrum 89 (2018) 10K121

[21] M. Osakabe *et al*., “Current Status of Large Helical Device and Its Prospect for Deuterium Experiment” *Fusion Sci. and Tech.* **72** (2017) 199-210

[22] M. Tokitani *et al*., “Microstructural characterization of mixed-material deposition layer on the LHD divertor tiles by using nano-geological diagnosis” *J. Nucl. Mater.* **438** (2013) S818-S821

[23] N. Ashikawa *et al.*, “Comparison of boronized wall in LHD and JT-60U” J. Nucl. Mater. **363-365**, (2007) 1352

[24] K. Nishimura *et al.*, “Effects of Boronization in LHD” *J. Plasma Fusion Res.* **79 (**2003) 1216

[25] R. D. Smirnov *et al*., “Modelling of dynamics and transport of carbon dust particles in tokamaks” *Plasma Phys. Control. Fusion* **49** (2007) 347-371

[26] M. Shoji *et al*., “Full-torus impurity transport simulation for optimizing plasma discharge operation using a multi-species impurity powder dropper in the large helical device” *Contrib. Plasma Phys.* **60** (2020) e201900101

[27] F. Nespoli et al., “First impurity powder injection experiments in LHD” *Nucl. Mater. Energy* **25** (2020) 100842

[28] M. Shoji *et al*., “Boron transport simulation using the ERO2.0 code for real-time wall conditioning in the large helical device” *Nucl. Mater. Energy* **25** (2020) 100853

[29] M. Osakabe et al., “Impact of carbon impurities on the confinement of high-ion-temperature discharges in the Large Helical Device” Plasma Physics and Controlled Fusion, vol.56, (2014) 095011.

[30] M.Z. Tokar et al., “A mechanism of ion temperature peaking by impurity pellet injection in a heliotron plasma” Plasma Physics and Controlled Fusion, vol.62, (2020) 075008.

[31] K. Ida et al., “The isotope effect on impurities and bulk ion particle transport in the Large Helical Device” Nucl. Fusion, 59 (2019) 056029.

[32] S.A. Bozhenkov et al., “High-performance plasmas after pellet injections in Wendelstein 7-X” *Nucl. Fusion* **60** (2020) 066011

[33] J Baldzuhn et al., “Enhanced energy confinement after series of pellets in Wendelstein 7-X” Plasma *Phys. Control. Fusion* **62** (2020) 05512

[34]T. Estrada et al., “Radial electric field and density fluctuations measured by Doppler reflectometry during the post-pellet enhanced confinement phase in W7-X” *Nucl. Fusion* **61** (2021) 046008

[35] T. Oishi et al., "Line identification of boron and nitrogen emissions in extreme- and vacuum-ultraviolet wavelength ranges in the impurity powder dropping experiments of the Large Helical Device and its application to spectroscopic diagnostics" *Plasma Sci. Technol.* **23** (2021) 084002

[36] Y. Nakamura et al., “A comprehensive study on impurity behavior in LHD long pulse discharges” *Nucl. Mater. Energy* **12** (2017) 124-132

[37] M. Kobayashi et al., “Edge impurity transport study in the stochastic layer of LHD and the scrape-off layer of HL-2A” *Nuclear Fusion*, vol. **53** (2013) 033011,

[38] S. Morita et al., “Effective screening of iron impurities in the ergodic layer of the Large Helical Device with a metallic first wall” *Nuclear Fusion*, vol. **53** (2013) 093017,

[39] J. Winter, “Wall conditioning in fusion devices and its influence on plasma performance,” *Plasma Phys. Control. Fusion*, **38**, no. 9, (1996) pp. 1503–1542

[40] O. I. Buzhinskij and Y. M. Semenets, “Review of in-Situ Boronization in Contemporary Tokamaks,” *Fusion Technol*., vol. **32**, (1997) pp. 1–13

[41] F. Bedoya et al., “Effect of boronization on plasma-facing graphite surfaces and its correlation with the plasma behavior in NSTX-U,” 2018 Nucl. Mater. Energy, vol. 17, pp. 211–216

[42] P. S. Krstic, J. P. Allain, F. J. Dominguez-Gutierrez, and F. Bedoya, “Unraveling the surface chemistry processes in lithiated and boronized plasma material interfaces under extreme conditions,” 2018 Matter and Radiation at Extremes, vol. 3, no. 4. Elsevier B.V., pp. 165–187

[43] R. Lunsford et al., “The impact of low-Z powder injection on intrinsic impurities in DIII-D” Preprint: 2020 IAEA Fusion Energy Conf. (2021) 10-15 May 2021 EX/P1-811

[44] M. Tokitani et al., “Plasma Wall interaction in long-pulse helium discharge in LHD - Microscopic modification of the wall surface and its impact on particle balance and impurity generation” *J. Nucl. Mater.* **463** (2015) 91-98

[45] Y. Hatano et al., “Measurement of deuterium and helium by glow-discharge optical emission spectroscopy for plasma-surface interaction studies” *Fusion Eng. and Design* **87** (2012) 1091-1094